Journal of Naval Architecture and Marine Engineering
June, 2007
http://jname.8m.net

DUFOUR AND SORET EFFECTS ON STEADY MHD FREE CONVECTION AND MASS TRANSFER FLUID FLOW THROUGH A POROUS MEDIUM IN A ROTATING SYSTEM

Nazmul Islam and Md. Mahmud Alam
Mathematics Discipline, Khulna University, Khulna-9208, Bangladesh, E-mail: alam_mahmud2000@yahoo.com

Abstract

The numerical studies are performed to examine the steady MHD free convection and mass transfer fluid flow through a continuously moving porous medium with thermal diffusion and diffusion thermo past a semi-infinite vertical porous plate in a rotating system. Impulsively started plate moving in its own plane is considered. With appropriate transformations the boundary layer equations are transformed into nonlinear ordinary differential equations. The local similarity solutions of the transformed dimensionless equations for the flow, heat and mass transfer characteristics are evaluated using shooting iteration technique. Numerical results are presented in the form of velocity, temperature and concentration within the boundary layer for different parameters entering into the analysis. Also the effects of the pertinent parameters on the local skin-friction coefficients and rate of heat transfer as well as rate of mass transfer in terms of the local Nusselt number and Sherwood number respectively are also discussed.

Keywords: MHD free convection, porous medium, rotation effect, Dufour effect, Soret effect.

NOMENCLATURE

x, y, z	Cartesian coordinates	G_r	Grashof number
f_w	Transpiration parameter	G_m	Modified Grashof number
u, v, w	Velocity components	K	Nondimensional permeability parameter
$v_0(x)$	Suction velocity	P_r	Prandtl number
$\mathbf{B}$	Magnetic field intensity	S_c	Schimidt number
$\mathbf{B}_0(x)$	Constant magnetic field intensity	S_r	Soret number
$\mathbf{J}=(J_x,J_y,J_z)$	Current density	D_f	Dufour number
Ω	Angular velocity	M	Magnetic parameter
k	Thermal conductivity of the medium	R	Rotation parameter
g_0	Gravitational acceleration	K'	Permeability of the porous medium
f′	Non-dimensional primary velocity	D_m	Coefficient of mass diffusivity
g	Non-dimensional secondary velocity	c_p	Specific heat at constant pressure
U_0	Uniform velocity	T_m	Mean fluid temperature

T	Temperature of the flow field	C_0	Mean concentration
T_w	Temperature at the plate	k_T	Thermal diffusion ratio
T_∞	Temperature of the fluid outside the boundary layer	c_s	Concentration susceptibility
C	Species concentration	N_u	Nusselt number
C_w	Concentration at the plate	S_h	Sherwood number
C_∞	Species concentration outside the boundary layer	(τ_x, τ_z)	Skin-friction coefficients

Greek

μ	Coefficient of viscosity	ρ	Fluid density
η	Similarity variable	σ'	Electrical conductivity
υ	Coefficient of kinematics viscosity	β	Coefficient of thermal expansion
θ	Dimensionless fluid temperature	β^*	Coefficient of concentration expansion
φ	Dimensionless fluid concentration		

1. **Introduction**

The science of magnetohydrodynamics (MHD) was concerned with geophysical and astrophysical problems for a number of years. In recent years the possible use of MHD is to affect a flow stream of an electrically conducting fluid for the purpose of thermal protection, braking, propulsion and control. From the point of applications, model studies on the effect of magnetic field on free convection flows have been made by several investigators. Some of them are Georgantopoulos (1979), Nanousis et al. (1980) and Raptis and Singh (1983). Along with the effects of magnetic field, the effect of transpiration parameter, being an effective method of controlling the boundary layer has been considered by Kafousias (1979) and Singh (1982). On the other hand, along with the free convection currents, caused by the temperature difference, the flow is also effected by the difference in concentrations on material constitution. Gebhart and Pera (1971) made extensive studies of such a combined heat and mass transfer flow to highlight the insight of the flow.

In the above mentioned works, the level of concentration of foreign mass is assumed very low so that the Soret and Dufour effects can be neglected. However, exceptions are observed therein. The Soret effect, for instance, has been utilized for isotope separation, and in mixture between gases with very light molecular weight (H_2, H_e) and of medium molecular weight (N_2, air). The Dufour effect was found to be of order of considerable magnitude such that it cannot be ignored (Eckert and Drake, 1972). In view of the importance of above mentioned effects, Kafoussias and Williams (1995) studied the Soret and Dufour effects on mixed free-forced convective and mass transfer boundary layer flow with temperature dependent viscosity. Anghel et al. (2000) vestigated the Dufour and Soret effects on free convection boundary layer flow over a vertical surface embedded in a porous medium. Quite recently, Alam and Rahman (2006) investigated the Dufour and Soret effects on mixed convection flow past a vertical porous flat plate with variable suction.

In consequence of the above studies, several investigators disclosed that the Coriolis force is very significant as compared to viscous and inertia forces occurring in the basic fluid equations. It is generally admitted that the Coriolis force due to Earth's rotation has a strong effect on the hydromagnetic flow in the Earth's liquid core. The study of such fluid flow problem is important due to its applications in various branches of geophysics astrophysics and fluid engineering. In light of, Singh and Singh (1989), Singh (1983,1984) and Raptis and Singh (1985) initiated a few studies by taking various aspects of the flow phenomena. From the point of application in Solar Physics and Cosmic fluid dynamics, it is important to consider the effects of the electromagnetic

and rotation forces on the flow. But no works of the simultaneous effects of the electromagnetic and rotation forces on the hydromagnetic free convection without Dufour and Soret effects have been reported in the literature.

Hence, our objective is to investigate the Dufour and Soret effects on steady MHD free convection and mass transfer flow through a porous medium past a semi-infinite vertical porous plate in a rotating system.

2. **Formulation of the problem and similarity analysis**

Consider a steady MHD free convection and mass transfer flow of an electrically conducting viscous fluid flow through a porous medium past a continuously moving semi-infinite vertical porous plate $y = 0$ in a rotating system. The flow is also assumed to be in the x-direction which is taken along the plate in the upward direction and y-axis is normal to it. Initially the fluid as well as the plate is at rest, after that the whole system is allowed to rotate with a constant angular velocity Ω about the y-axis. The temperature and the species concentration at the plate are constantly raised from T_w and C_w to T_∞ and C_∞ respectively, which are thereafter maintained constant. T_∞ and C_∞ are the temperature and species concentration of the uniform flow respectively. A uniform magnetic field $\mathbf{B}$ is taken to be acting along the $y-axis$ which is assumed to be electrically non-conducting. We assumed that the magnetic Reynolds number of the flow is taken to be small enough so that the induced magnetic field is negligible in comparison with applied one (Pai, 1962), so that $\mathbf{B} = (0, B_0, 0)$ and the magnetic lines of force are fixed relative to the fluid. The equation of conservation of charge $\nabla.\mathbf{J} = 0$ gives $J_y =$ constant, where the current density $\mathbf{J} = (J_x, J_y, J_z)$. Since the plate is electrically non-conducting, this constant is zero and hence $J_y = 0$ at the plate and hence zero everywhere. The physical configuration considered here is shown in the following Fig. 1.

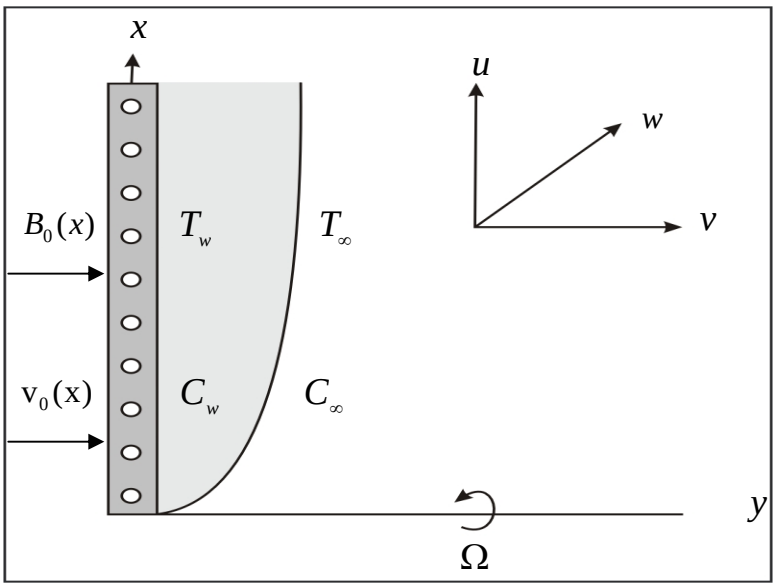

Fig. 1. Physical configuration and coordinate system.

Thus accordance with the above assumptions relevant to the problem and Boussinesq's approximation, the basic boundary layer equations are given by

The continuity equation: $$\frac{\partial u}{\partial x} + \frac{\partial v}{\partial y} = 0 \qquad (1)$$

The momentum equations:

$$u\frac{\partial u}{\partial x}+v\frac{\partial u}{\partial y}=\upsilon\frac{\partial^2 u}{\partial y^2}+g_0\beta\left(T-T_\infty\right)+g_0\beta^*\left(C-C_\infty\right)+2\Omega w-\frac{\upsilon}{K'}u-\frac{\sigma' B_0{}^2 u}{\rho} \tag{2}$$

$$u\frac{\partial w}{\partial x}+v\frac{\partial w}{\partial y}=\upsilon\frac{\partial^2 w}{\partial y^2}-2\Omega u-\frac{\upsilon}{K'}w-\frac{\sigma' B_0{}^2 w}{\rho} \tag{3}$$

The energy equation:

$$u\frac{\partial T}{\partial x}+v\frac{\partial T}{\partial y}=\frac{k}{\rho c_p}\frac{\partial^2 T}{\partial y^2}+\frac{D_m k_T}{c_s c_p}\frac{\partial^2 C}{\partial y^2} \tag{4}$$

The concentration equation:

$$u\frac{\partial C}{\partial x}+v\frac{\partial C}{\partial y}=D_m\frac{\partial^2 C}{\partial y^2}+\frac{D_m k_T}{T_m}\frac{\partial^2 T}{\partial y^2} \tag{5}$$

The boundary conditions for the present problem are given by:

$$\left.\begin{aligned}&u=U_0, v=v_0(x), w=0, T=T_w, C=C_w \text{ at } y=0\\&u=0, v=0, w=0, T\to T_\infty, C\to C_\infty \text{ at } y\to\infty\end{aligned}\right\} \tag{6}$$

where all physical quantities are defined in the nomenclature.

We now introduce the following dimensionless variables

$$\begin{cases}\eta=y\sqrt{\dfrac{U_0}{2\upsilon x}}\\ f'(\eta)=\dfrac{u}{U_0}\\ g(\eta)=\dfrac{w}{U_0}\\ \theta(\eta)=\dfrac{T-T_\infty}{T_w-T_\infty}\\ \phi(\eta)=\dfrac{C-C_\infty}{\bar{x}\left(C_0-C_\infty\right)}\end{cases} \tag{7}$$

Now for reasons of similarity, the plate concentration is assumed to be

$$C_w(x)=C_\infty+\bar{x}\left(C_0-C_\infty\right), \tag{8}$$

where C_0 is considered to be mean concentration and $\bar{x}=\dfrac{xU_0}{\upsilon}$.

Introducing the relations (7)-(8) into the equations (2)-(5), we obtain the following local similarity equations

$$f'''+ff''+G_r\theta+G_m\phi-Kf'-Mf'-2Rg=0 \tag{9}$$

$$g''+fg'-Kg-Mg+2Rf'=0 \tag{10}$$

$$\theta''+P_r f\theta'+P_r D_f\phi''=0 \tag{11}$$

$$\phi''-2S_c f'\phi+S_c f\phi'+S_c S_r\theta''=0 \tag{12}$$

where $G_r = \frac{g_0\beta(T_w - T_\infty)}{U_0^{\,2}}2x, G_m = \frac{g_0\beta^*(C_0 - C_\infty)}{\upsilon U_0}2x^2$,

$K = \frac{2\upsilon x}{K'U_0}, M = \frac{\sigma' B_0^{\,2}2x}{\rho U_0}, R = \frac{2\Omega x}{U_0}, P_r = \frac{\rho\upsilon c_p}{k}, D_f = \frac{D_m k_T}{c_s c_p \upsilon}\frac{xU_0}{\upsilon}\frac{(C_0 - C_\infty)}{(T_w - T_\infty)}$,

$S_c = \frac{\upsilon}{D_m}$ and $S_r = \frac{D_m k_T}{\upsilon T_m}\frac{\upsilon}{xU_0}\frac{(T_w - T_\infty)}{(C_0 - C_\infty)}$.

The corresponding boundary conditions are

$$\left.\begin{aligned} f = f_w, f' = 1, g = 0, \theta = 1, \phi = 1 \, at \, \eta = 0 \\ f' = 0, g = 0, \theta = 0, \phi = 0 \, as \, \eta \to \infty \end{aligned}\right\} \quad (13)$$

where $f_w = -v_0(x)\sqrt{\frac{2x}{\upsilon U_0}}$ is taken to be transpiration parameter.

3. Skin-friction coefficients, Nusselt number and Sherwood number

The quantities of physical interest are the skin friction coefficients, the Nusselt number and the Sherwood number. The equations defining the wall skin frictions are

$\tau_x = \mu\left(\frac{\partial u}{\partial y}\right)_{y=0}$, $\tau_z = \mu\left(\frac{\partial w}{\partial y}\right)_{y=0}$ which are proportional to $\left(\frac{\partial^2 f}{\partial \eta^2}\right)_{\eta=0}$ and $\left(\frac{\partial g}{\partial \eta}\right)_{\eta=0}$.

The Nusselt number denoted by N_u is proportional to $-\left(\frac{\partial T}{\partial y}\right)_{y=0}$, hence we have

$N_u \infty - \theta'(0)$.

The Sherwood number S_h is proportional to $-\left(\frac{\partial C}{\partial y}\right)_{y=0}$, hence we have

$S_h \infty - \varphi'(0)$.

The numerical values of the local skin-friction coefficients, the local Nusselt number and the local Sherwood number are sorted in Tables 1-3.

4. **Numerical Solution**

The set of non-linear ordinary differential equations (9)-(12) with boundary conditions (13) have been solved by using sixth order Runge-Kutta method along with the Nacthsheim-Swigert (1965) shooting iteration technique.

5. **Results and Discussion**

In this paper, the effect of different parameters entering into steady two-dimensional MHD free convection and mass transfer fluid flow through a porous medium past a continuously moving semi-infinite vertical porous plate $y = 0$ in a rotating system has been investigated using Nacthsheim-Swigert shooting iteration technique.

For the purpose of discussing the effects of various parameters on the flow behavior, some numerical calculations have been carried out for non-dimensional primary velocity $f'(\eta)$, secondary velocity $g(\eta)$, temperature $\theta(\eta)$ and concentration $\varphi(\eta)$.

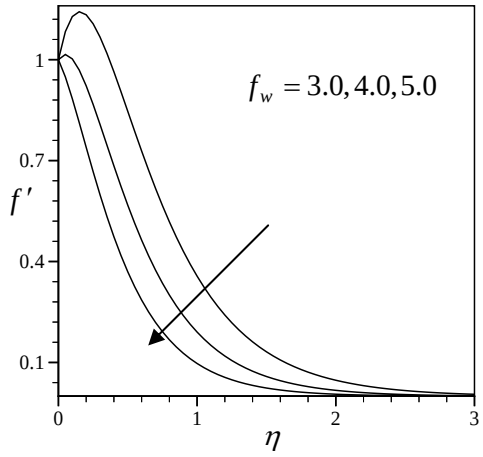

Fig. 2: Primary velocity profiles for different values of f_w with $G_r = 10.0$, $G_m = 4.0$, $M = 0.5$, $R = 0.2$, $P_r = 0.71$, $S_r = 1.0$, $S_c = 0.6$, $D_f = 0.2$, $K = 0.5$.

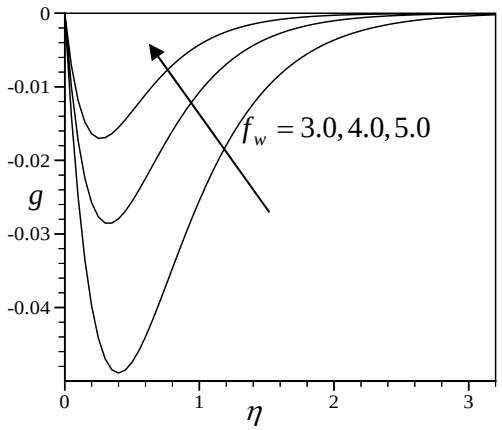

Fig. 3: Secondary velocity profiles for different values of f_w with $G_r = 10.0$, $G_m = 4.0$, $M = 0.5$, $R = 0.2$, $P_r = 0.71$, $S_r = 1.0$, $S_c = 0.6$, $D_f = 0.2$, $K = 0.5$.

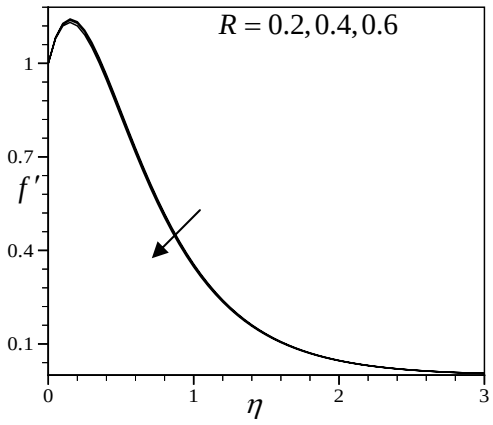

Fig. 4: Primary velocity profiles for different values of R with $f_w = 3.0$, $G_r = 10.0$, $G_m = 4.0$, $M = 0.5$, $P_r = 0.71$, $S_r = 1.0$, $S_c = 0.6$, $D_f = 0.2$, $K = 0.5$.

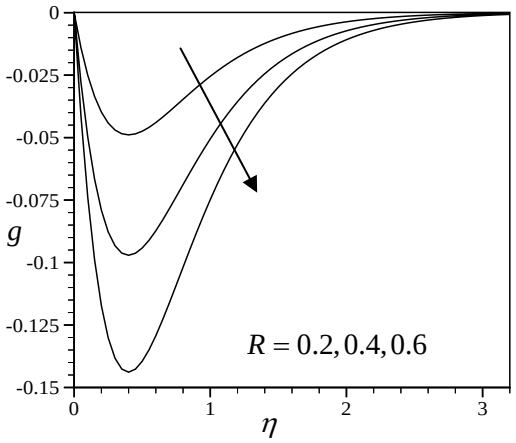

Fig. 5: Secondary velocity profiles for different values of R with $f_w = 3.0$, $G_r = 10.0$, $G_m = 4.0$, $M = 0.5$, $P_r = 0.71$, $S_r = 1.0$, $S_c = 0.6$, $D_f = 0.2$, $K = 0.5$.

The velocity profiles for x and z components of velocity, commonly known as non-dimensional primary (f') and secondary (g) velocities, are shown in Figs. 2 - 17 for different values of suction parameter (v_0), the magnetic parameter (M), the rotation parameter (R), the Prandtl number (P_r), the Soret number (S_r), the Schmidt number (S_c), the Dufour number (D_f) and the permeability parameter (K) and for fixed values of Grashof number (G_r) and modified Grashof number (G_m).

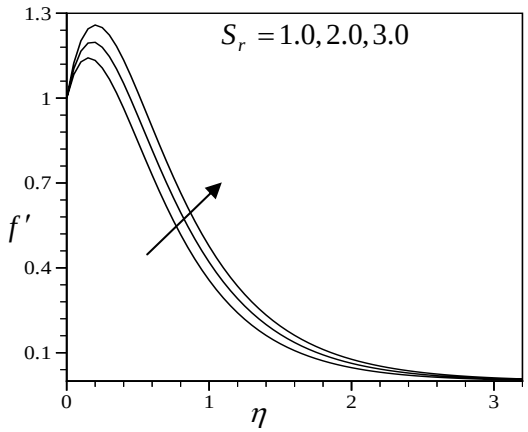

Fig. 6: Primary velocity profiles for different values of S_r with $f_w = 3.0$, $G_r = 10.0$, $G_m = 4.0$, $M = 0.5$, $R = 0.2$, $P_r = 0.71$, $S_c = 0.6$, $D_f = 0.2$, $K = 0.5$.

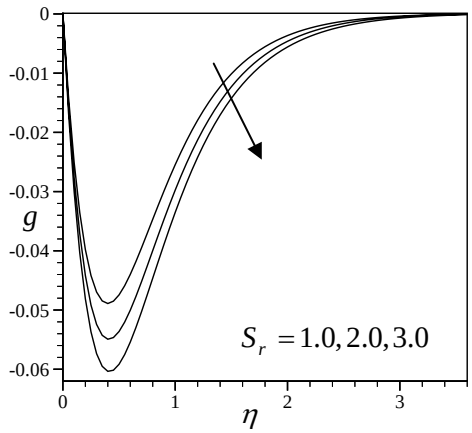

Fig. 7: Secondary velocity profiles for different values of S_r with $f_w = 3.0$, $G_r = 10.0$, $G_m = 4.0$, $M = 0.5$, $R = 0.2$, $P_r = 0.71$, $S_c = 0.6$, $D_f = 0.2$, $K = 0.5$.

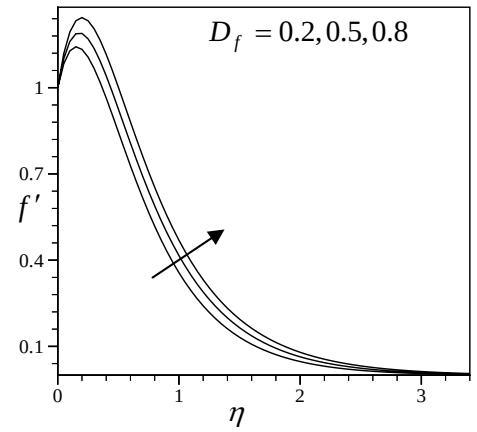

Fig. 8: Primary velocity profiles for different values of D_f with $f_w = 3.0$, $G_r = 10.0$, $G_m = 4.0$, $M = 0.5$, $R = 0.2$, $P_r = 0.71$, $S_r = 1.0$, $S_c = 0.6$, $K = 0.5$.

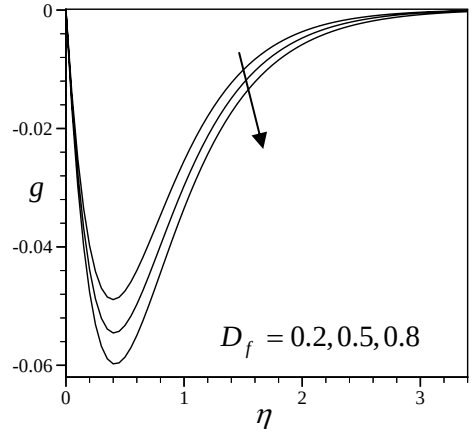

Fig. 9: Secondary velocity profiles for different values of D_f with $f_w = 3.0$, $G_r = 10.0$, $G_m = 4.0$, $M = 0.5$, $R = 0.2$, $P_r = 0.71$, $S_r = 1.0$, $S_c = 0.6$, $K = 0.5$.

For Prandtl number (P_r), three values $0.71, 1.0$ and 7.0 which represent air at 20 deg C, electrolytic solution such as salt water and water respectively. The values $0.22, 0.60$ and 0.75 of the Schmidt number (S_c) are also considered for they represent specific conditions of the flow. In particular, 0.22 corresponds to Hydrogen while 0.60 corresponds to water vapor that represents a diffusivity chemical species of most common interest in air and the value 0.75 represent Oxygen. In the calculations f_w, M , R , S_r , D_f , K and G_m are chosen arbitrarily.

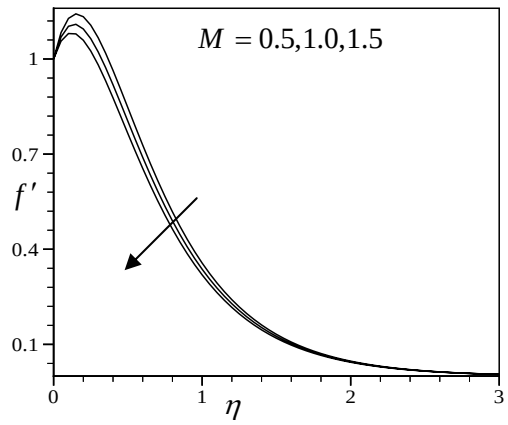

Fig. 10: Primary velocity profiles for different values of M with $f_w = 3.0$, $G_r = 10.0$, $G_m = 4.0$, $R = 0.2$, $P_r = 0.71$, $S_r = 1.0$, $S_c = 0.6$, $D_f = 0.2$, $K = 0.5$.

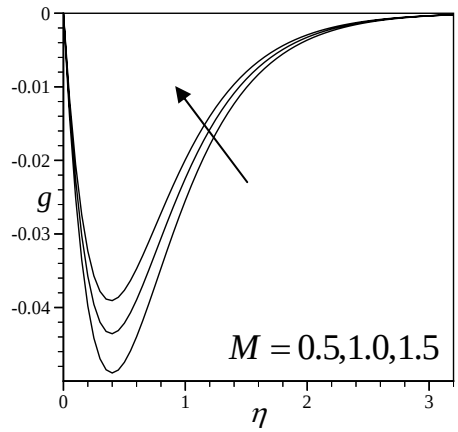

Fig. 11: Secondary velocity profiles for different values of M with $f_w = 3.0$, $G_r = 10.0$, $G_m = 4.0$, $R = 0.2$, $P_r = 0.71$, $S_r = 1.0$, $S_c = 0.6$, $D_f = 0.2$, $K = 0.5$.

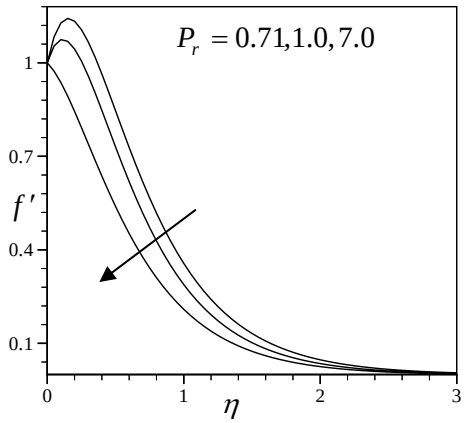

Fig. 12: Primary velocity profiles for different values of P_r with $f_w = 3.0$, $G_r = 10.0$, $G_m = 4.0$, $M = 0.5$, $R = 0.2$, $S_r = 1.0$, $S_c = 0.6$, $D_f = 0.2$, $K = 0.5$.

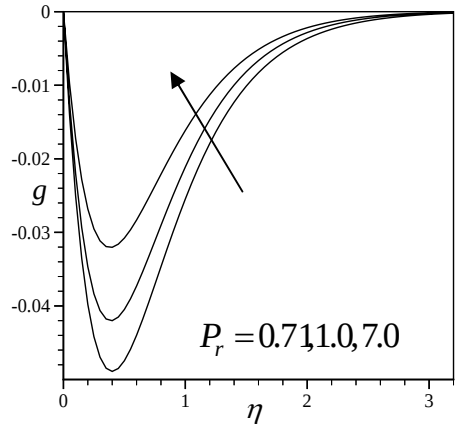

Fig. 13: Secondary velocity profiles for different values of P_r with $f_w = 3.0$, $G_r = 10.0$, $G_m = 4.0$, $M = 0.5$, $R = 0.2$, $S_r = 1.0$, $S_c = 0.6$, $D_f = 0.2$, $K = 0.5$.

With the above mentioned flow parameters, it is observed from Figs. 2 and 3 that an increase in the suction parameter f_w leads to decrease in the primary velocity and to increase the secondary velocity.

The variations of the primary and secondary velocities for different values of rotation parameter R are shown in Figs. 4 & 5. From these figures it is observed that the rotation parameter R has a minor decreasing effect on the primary velocity while it has quite a larger decreasing effect on the secondary velocity. In Figs. 6 & 7 and 8 & 9, the variations of the primary and secondary velocities for different

values of Soret number S_r and Dufour number D_f are shown respectively. From these figures it is observed that the primary velocity increases with the increase of Soret number S_r and Dufour number D_f. The effects of Soret number S_r and Dufour number D_f on the secondary velocity are opposite to that of the primary velocity. In Figs. 10 & 11, 12 & 13, 14 & 15 and 16 & 17, the variations of the primary and secondary velocities for different values of magnetic parameter M, Prandtl number P_r, Schmidt number S_c and permeability parameter K are shown respectively. It is observed from these figures that the magnetic parameter M has a decreasing effect on the primary velocity and increasing effect on the secondary velocity. It is also seen from these figures that the primary velocity decreases while the secondary velocity increases with the increase of Prandtl number P_r. The same effects are observed in the case of Schmidt number S_c and permeability parameter K. The effects of various parameters on non-dimensional temperature are shown in Figs. 18-20. It is observed from Fig. 18 that the temperature decreases with the increase of suction parameter f_w increase. In Fig. 19, the temperature profiles for different values of Dufour number D_f are shown. It is observed from this figure that the Dufour number D_f has an increasing effect. In Fig. 20, the temperature profiles for different values of Prandtl number P_r are shown. This figure revels that the Prandtl number P_r has a large decreasing effect on temperature.The effects of various parameters on the concentration field are shown in Figs. 21 - 24. It is observed from Fig. 21 that the concentration decreases as the suction parameter f_w increase. The concentration profiles for different values of Soret number S_r are shown in Fig. 22. The figure shows that the concentrations increases as the Soret number S_r increase.

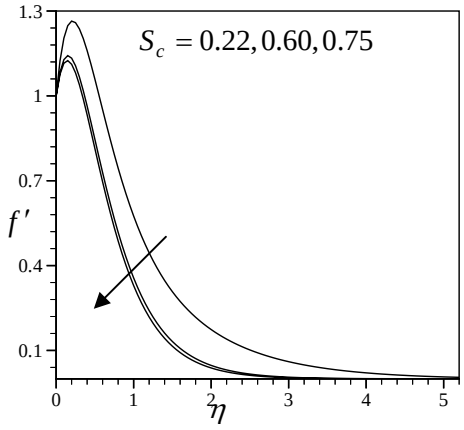

Fig. 14: Primary velocity profiles for different values of S_c with $f_w = 3.0$, $G_r = 10.0$, $G_m = 4.0$, $M = 0.5$, $R = 0.2$, $P_r = 0.71$, $S_r = 1.0$, $D_f = 0.2$, $K = 0.5$.

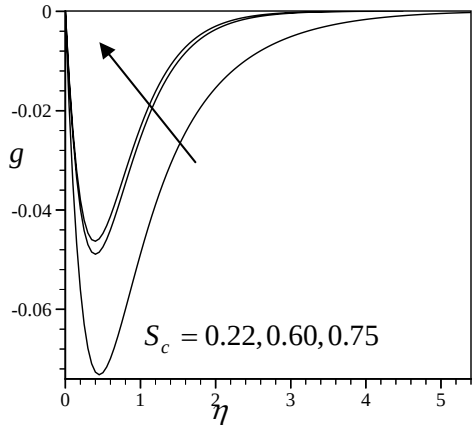

Fig. 15: Secondary velocity profiles for different values of S_c with $f_w = 3.0$, $G_r = 10.0$, $G_m = 4.0$, $M = 0.5$, $R = 0.2$, $P_r = 0.71$, $S_r = 1.0$, $D_f = 0.2$, $K = 0.5$.

In Figs. 23 and 24, the concentration profiles for different values of Prandtl number P_r and Schmidt number S_c are shown respectively. It is observed from these figures that the concentration increases as the Prandtl number P_r increase while the concentration decreases as the Schmidt number S_c increase. Finally, the effects of various parameters on the components of the skin friction coefficient τ_x and τ_z, the Nusselt number N_u and the Sherwood number S_h are shown in Tables 1-3.

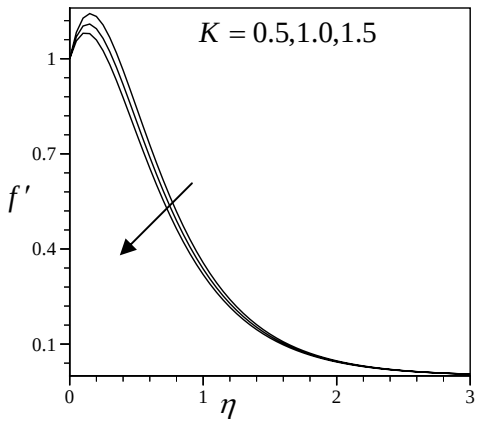

Fig. 16: Primary velocity profiles for different values of K with $f_w = 3.0$, $G_r = 10.0$, $G_m = 4.0$, $M = 0.5$, $R = 0.2$, $P_r = 0.71$, $S_r = 1.0$, $S_c = 0.6$, $D_f = 0.2$.

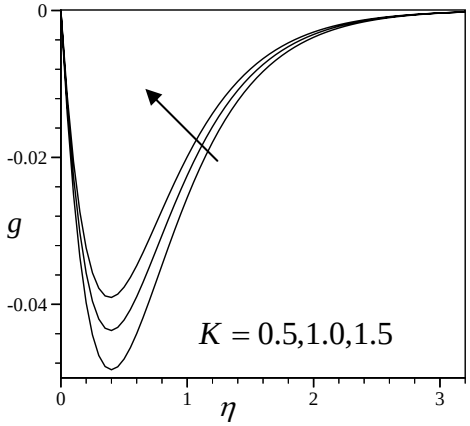

Fig. 17: Secondary velocity profiles for different values of K with $f_w = 3.0$, $G_r = 10.0$, $G_m = 4.0$, $M = 0.5$, $R = 0.2$, $P_r = 0.71$, $S_r = 1.0$, $S_c = 0.6$, $D_f = 0.2$

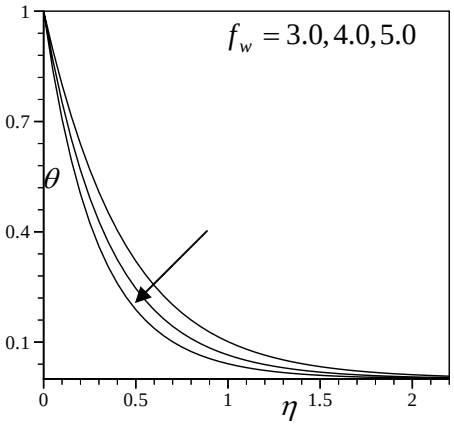

Fig. 18: Temperature profiles for different values of f_w with $G_r = 10.0$, $G_m = 4.0$, $M = 0.5$, $R = 0.2$, $P_r = 0.71$, $S_r = 1.0$, $S_c = 0.6$, $D_f = 0.2$, $K = 0.5$.

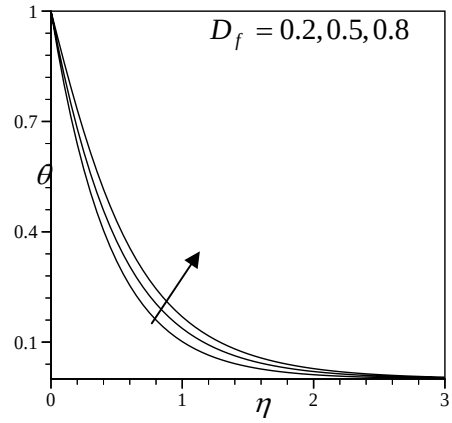

Fig. 19: Temperature profiles for different values of D_f with $f_w = 3.0$, $G_r = 10.0$, $G_m = 4.0$, $M = 0.5$, $R = 0.2$, $P_r = 0.71$, $S_r = 1.0$, $S_c = 0.6$, $K = 0.5$.

From Table 1, we observe that the skin-friction component τ_x decreases with the increase of suction parameter f_w, but the skin-friction component τ_z, the Nusselt number N_u and the Sherwood number S_h increase with the increase of suction parameter f_w. It is also observed from this table that the skin-friction component τ_x, the Nusselt number N_u and Sherwood number S_h decrease with the increase of magnetic parameter M, while the skin-friction component τ_z increases with the increase of magnetic parameter M.

Again, from Table 2, we observe that the skin-friction components τ_x and τ_z, the Nusselt number N_u and the Sherwood number S_h decrease with the increase of rotation parameter R. It is also observed from this table that the skin-friction component τ_x and the Nusselt number N_u increase while the skin-friction component τ_z and the Sherwood number S_h decrease with the increase of Soret number S_r.

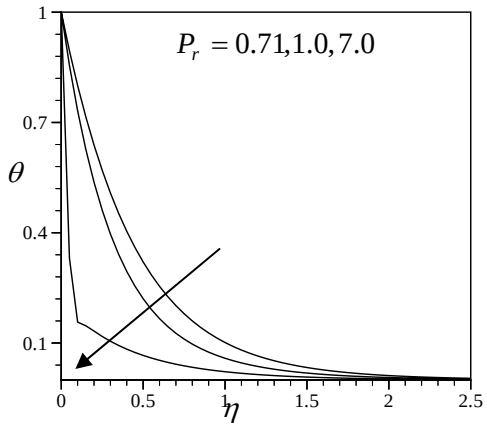

Fig. 20: Temperature profiles for different values of P_r with $f_w = 3.0$, $G_r = 10.0$, $G_m = 4.0$, $M = 0.5$, $R = 0.2$, $S_r = 1.0$, $S_c = 0.6$, $D_f = 0.2$, $K = 0.5$.

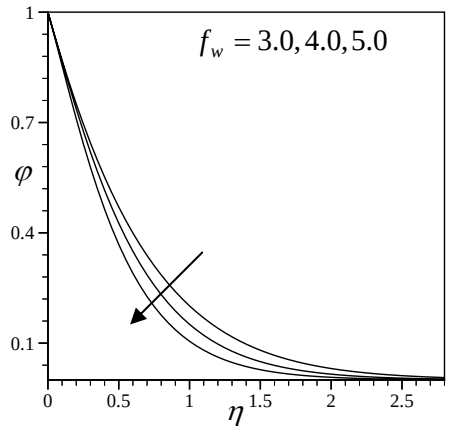

Fig. 21: Concentration profiles for different values of f_w with $G_r = 10.0$, $G_m = 4.0$, $M = 0.5$, $R = 0.2$, $P_r = 0.71$, $S_r = 1.0$, $S_c = 0.6$, $D_f = 0.2$, $K = 0.5$.

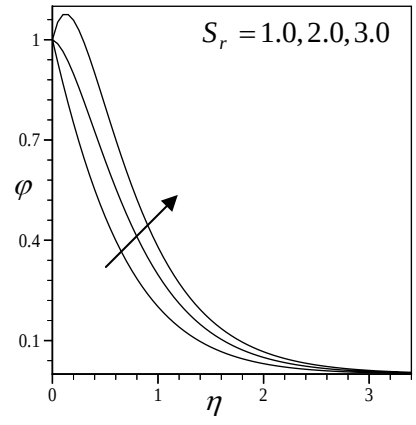

Fig. 22: Concentration profiles for different values of S_r with $f_w = 3.0$, $G_r = 10.0$, $G_m = 4.0$, $M = 0.5$, $R = 0.2$, $P_r = 0.71$, $S_c = 0.6$, $D_f = 0.2$, $K = 0.5$.

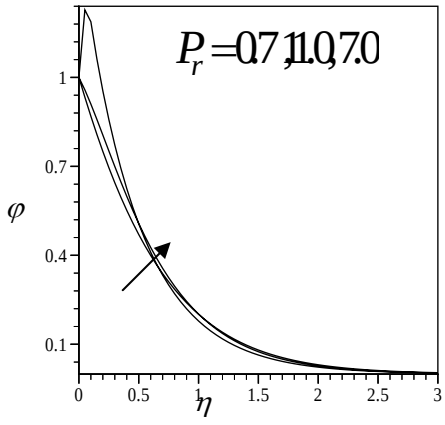

Fig. 23: Concentration profiles for different values of P_r with $f_w = 3.0$, $G_r = 10.0$, $G_m = 4.0$, $M = 0.5$, $R = 0.2$, $S_r = 1.0$, $S_c = 0.6$, $D_f = 0.2$, $K = 0.5$.

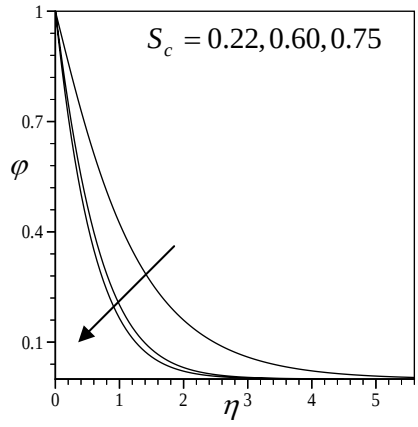

Fig. 24: Concentration profiles for different values of S_c with $f_w = 3.0$, $G_r = 10.0$, $G_m = 4.0$, $M = 0.5$, $R = 0.2$, $P_r = 0.71$, $S_r = 1.0$, $D_f = 0.2$, $K = 0.5$.

From Table 3, we observe that the skin-friction component τ_x and the Sherwood number S_h increase while the skin-friction component τ_z and the Nusselt number N_u decrease owing to the increase of Dufour number D_f . It is also seen from this table that the skin-friction component τ_x , the Nusselt number N_u and the Sherwood number S_h decrease while the skin-friction component τ_z increases with the increase of permeability parameter K .

Table 1: Numerical values of τ_x, τ_z, N_u and S_h for $P_r = 0.71$, $G_r = 10.0$, $G_m = 4.0$, $R = 0.2$, $S_r = 1.0$, $S_c = 0.6$, $D_f = 0.2$ and $K = 0.5$.

f_w	M	τ_x	τ_z	N_u	S_h
3.0	0.5	2.1183684	-0.3123093	2.2126436	1.3606514
4.0	0.5	0.6630225	-0.2322516	2.8415285	1.3736072
5.0	0.5	-0.8398383	-0.1720828	3.4941526	1.3843751
3.0	1.0	1.8034374	-0.2837792	2.2074190	1.3379786
3.0	1.5	1.5115707	-0.2596410	2.2026285	1.3168868

Table 2: Numerical values of τ_x, τ_z, N_u and S_h for $f_w = 0.5$, $G_r = 10.0$, $G_m = 4.0$, $M = 0.5$, $P_r = 0.71$, $S_c = 0.6$, $D_f = 0.2$ and $K = 0.5$.

R	S_r	τ_x	τ_z	N_u	S_h
0.2	1.0	2.1183684	-0.3123093	2.2126436	1.3606514
0.4	1.0	2.0825316	-0.6208549	2.2119861	1.3572153
0.6	1.0	2.0241833	-0.9220832	2.2107869	1.3517746
0.2	2.0	2.5626587	-0.3425054	2.4041973	0.1109341
0.2	3.0	2.9919283	-0.3699451	2.6305160	-1.3989729

Table 3: Numerical values of τ_x, τ_z, N_u and S_h for $f_w = 0.5$, $G_r = 10.0$, $G_m = 4.0$, $P_r = 0.71$, $R = 0.2$, $M = 0.5$, $S_r = 1.0$ and $S_c = 0.6$.

D_f	K	τ_x	τ_z	N_u	S_h
0.2	0.5	2.1183684	-0.3123093	2.2126436	1.3606514
0.5	0.5	2.5017350	-0.3402315	1.8900020	1.5829858
0.8	0.5	2.8887150	-0.3663611	1.4347118	1.8786190
0.2	1.0	1.8034374	-0.2837792	2.2074190	1.3379786
0.2	1.5	1.5115707	-0.2596410	2.2026285	1.3168868

References

Alam, M. S. and Rahman, M. M. (2006): Dufour and Soret Effects on Mixed Convection Flow past a Vertical Porous Flat Plate with Variable Suction, *Nonlinear analysis: Modeling and Control*, **11**, 1.

Anghel, M., Takhur, H. S. and Pop, I. (2000): Dufour and Soret Effects on Free Convection Boundary-layer over a Vertical Surface Embedded in a Porous Medium, *Studia Universitatis Babes-Bolyai. Mathematica*, **XLV(4),** 11.

Eckert, E. R. G. and Drake, R. M. (1972): *Analysis of Heat and Mass Transfer,* McGraw-Hill Book Co., New York.

Georgantopoulos, G. A. (1979): Effects of Free Convection on the Hydromagnetic Accelerated Flow Past a Vertical Porous Limiting Surface. *Astrophysics and Space Science,* **65**, 433.

Gebhart, B. and Pera, L. (1971): The Nature of Vertical Convection Flows Resulting from Combined Buoyancy Effects of the Thermal and Mass Diffusion Nature, *International Journal of Heat and Mass Transfer,* **14,** 2025.

Kafousias, N. G., Nanousis, N. and Georgantopoulos, G. A. (1979): Free Convection Effects on the Stokes Problem for an Infinite Vertical Limiting Surface with Constant Suction, *Astrophysics and Space Science,* **64,** 391.

Kafoussias, N. G. and Williams, E. M. (1995): Thermal-diffusion and Diffusion-thermo Effects on Mixed Free-forced Convective and Mass Transfer Boundary Layer Flow with Temperature Dependent Viscosity, *Internatinal Journal of Engineering Science,* **33**, 1369.

Nachtssheim, P. R. and Swigert, P. (1965): Satisfaction of the Asymptotic Boundary Conditions in Numerical Solution of the System of Nonlinear Equations of Boundary Layer Type, NASA TND-3004.

Nanousis, N., Georgantopoulos, G. A. and Papaioannou, A. (1980): Hydromagnetic Free Convection Flow in the Stokes Problem for a Porous Vertical Limiting Surface with Constant Suction, *Astrophysics and Space Science,* **70,** 377.

Pai, S. I. (1962): *Magnetogasdynamics and Plasma dynamics*, Springier Verlag, NewYork.Raptis, A. and Singh, A. K. (1983): MHD Free Convection Flow Past an Accelerated Vertical Plate, *International Communications in Heat and Mass Transfer,* **10**, 313.

Raptis, A. and Singh, A. K. (1985): Rotation Effects on MHD Free Convection Flow Past an Accelerated Vertical Plate, *Mechanical Resulation Communication*, **12**, 31.

Singh, A. K. (1982): MHD Free Convection Flow in the Stokes Problem for a Porous Vertical Plate, *Astrophysics and Space Science,* **87,** 455.

Singh, A. K. and Singh, J. N. (1989): Transient MHD Free Convection in a Rotating System, *Astrophysics and Space Science,* **162,** 85.

Singh, A. K. (1983): MHD Free Convection Flow in the Stokes Problem for a Vertical Porous Plate in a Rotating System, *Astrophysics and Space Science,* **95,** 283.

Singh, A. K. (1984a): Hydromagnetic Free Convection Flow Past an Impulsively Started Vertical Plate in a Rotating System, *International Communications in Heat and Mass Transfer*, **11**, 349.

Singh, A. K. (1984b): Stokes Problem for a Porous Vertical Plate with Heat Sinks by Finite Difference Method, *Astrophysics and Space Science,* **103,** 55.